Biological Oxygen-dosed Activated Carbon (BODAC) filters – A bioprocess for ultrapure water production removing organics, nutrients and micropollutants

Bernadet, Olga; Larasati, Amanda; van Veelen, H. Pieter J.; Euverink, Gert Jan Willem; Gagliano, Maria Cristina

Published in:
Journal of hazardous materials

DOI:
10.1016/j.jhazmat.2023.131882

Publication date:
2023

Journal of Hazardous Materials 458 (2023) 131882

Contents lists available at ScienceDirect

Journal of Hazardous Materials

journal homepage: www.elsevier.com/locate/jhazmat

Biological Oxygen-dosed Activated Carbon (BODAC) filters – A bioprocess for ultrapure water production removing organics, nutrients and micropollutants

Olga Bernadet [a,b], Amanda Larasati [a], H. Pieter J. van Veelen [a], Gert Jan Willem Euverink [b,*], Maria Cristina Gagliano [a]

[a] Wetsus, Center of European Excellence in Water Technology, Oostergoweg 9, 8911 MA Leeuwarden, the Netherlands
[b] Engineering and Technology Institute Groningen (ENTEG), University of Groningen, Nijenborgh 4, Groningen, the Netherlands

HIGHLIGHTS

- BODAC filters were operated for 11 years without carbon regeneration or replacement.
- In 2 years monitoring, BODAC filters removed soluble organics, nitrogen species, and manganese.
- BODAC filters removed some organic micropollutants with high efficiency (≥70 %).
- BODAC granules were covered by biofilm and inorganic depositions rich in Mn, Ca, and Fe.
- BODAC activity connected to nitrifying and manganese-oxidizing bacteria in the granule biofilms.

GRAPHICAL ABSTRACT

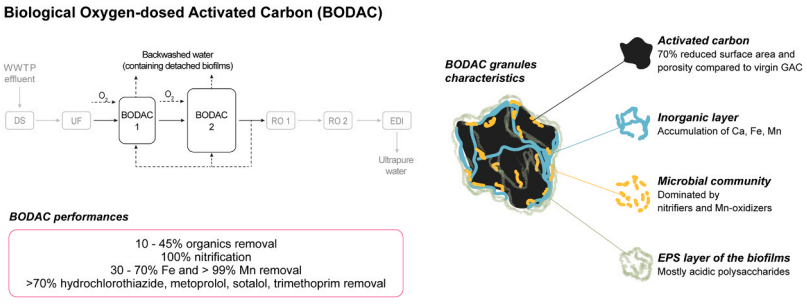

ARTICLE INFO

Editor: <Peiying Hong>

Keywords:
Biological activated carbon
Organic micropollutants
Biofilms
Nitrification
Manganese removal

ABSTRACT

Biological oxygen-dosed activated carbon (BODAC) filters in an Ultrapure water plant were demonstrated to have the potential to further treat secondary wastewater treatment effluent. The BODAC filters were operated for 11 years without carbon regeneration or replacement, while still functioning as pre-treatment step to reverse osmosis (RO) membranes by actively removing organic micropollutants (OMPs) and foulants. In this study, the removal of nutrients and 13 OMPs from secondary wastewater treatment effluent was investigated for 2 years and simultaneously, the granules' characterization and microbial community analysis were conducted to gain insights behind the stable long-term operation of the BODAC filters. The results showed that the BODAC granules' surface area was reduced by ~70 % of what is in virgin carbon granules and covered by biofilm and inorganic depositions. The BODAC filters reduced the concentration of soluble organics, mainly proteins, performed as an effective nitrification system, and almost completely removed manganese. During the 2 years of observation, the filters consistently removed some OMPs such as hydrochlorothiazide, metoprolol, sotalol, and trimethoprim by at least 70 %. Finally, through microbial community analysis, we found that nitrifying and manganese-oxidizing bacteria were detected in high relative abundance on BODAC granules, supporting BODAC performance in removing OMPs and manganese as well as converting nitrogenous species in the water.

* Correspondence to: Engineering and Technology Institute Groningen (ENTEG), University of Groningen, Nijenborgh 4, Groningen 9747 AG, the Netherlands.
E-mail address: g.j.w.euverink@rug.nl (G.J.W. Euverink).

https://doi.org/10.1016/j.jhazmat.2023.131882
Received 24 February 2023; Received in revised form 14 June 2023; Accepted 15 June 2023
Available online 17 June 2023

1. Introduction

Water reuse from the effluent of wastewater treatment plants (WWTPs) has been increasingly discussed, and several advanced technologies have been developed for this purpose [1]. The Ultrapure water (UPW) factory in Emmen, the Netherlands (NL), is a successful example of a wastewater reuse technology where the secondary effluent of a nearby WWTP is treated into UPW with low conductivity (<0.2 μS/cm), which is used for steam injection in an oil extraction process [2]. The UPW factory implements a number of consecutive water treatment steps, namely drum sieves, ultrafiltration (UF) membranes, a series of Biological Oxygen-dosed Activated Carbon (BODAC) filters, Reverse Osmosis (RO) membranes, and electro-deionization units (EDI) [2] as depicted in Fig. 1. The presence of organics, e.g., biopolymers and humic substances, and other contaminants in WWTPs secondary effluents can lead to (bio)fouling of the RO membranes [3,4].

Normally, depending on the quality of the water source and the potential foulants present, pre-treatment(s) is applied before RO membranes to prevent (bio)fouling [5,6]. UF pre-treatment is usually applied to remove particles, microorganisms, and organic matter [7]. However, UF alone is not economically viable for its cleaning and maintenance needs, and because it does not remove the smaller and soluble organic matter molecules, which often cause biofouling of RO units [8]. Biological activated carbon (BAC) filtration applied as RO pre-treatment effectively reduces concentration of potential foulants [4]. However, this pretreatment is often not able to remove organics (i.e., soluble extracellular polymeric substances (sEPS) and humic-like substances) from secondary WWTP effluents which are highly resistant to further biodegradation [9]. BODAC filters are BAC reactors where oxygen at a high concentration is dosed regularly to keep an oxic condition along the filters' height. Regular oxygen dosing has the aim of avoiding oxygen deprivation, which could cause biomass decay and stimulate microbial kinetics, and therefore the breakdown of recalcitrant organics [10,11].

In the UPW plant, BODAC filters were installed together with UF as a pre-treatment line to prevent (bio)fouling in the RO units [12]. As a result, after more than 11 years of operation of the UPW factory, the original RO units were still in operation and never subjected to major fouling issues [13]. The hypothesis is that the application of combined UF and BODAC filters as a pre-treatment likely led to the removal of the whole range of (bio)fouling precursors, limiting their accumulation and/or microbial growth on the RO membranes [12]. During this period, the BODAC filters has the potential for removing organic micropollutants (OMPs) from the treated WWTP effluent to a great extent (up to 99 %) [13]. Removal of OMPs by BODAC is of importance because WWTP effluents are considered as major source of OMPs in the environment [14,15] and the efficient removal of OMPs in WWTP effluents is commonly thought of as the bottleneck in most wastewater reclamation projects [16].

The removal of organics, nutrients, and OMPs by conventional BAC granules is usually achieved by a combination of adsorption and the activity of the biofilm growing on the carbon surface [17], the latter contributing to the so-called carbon bio-regeneration by metabolizing the adsorbed compounds [18]. The increased availability of dissolved oxygen in BODAC filters can also stimulate such bio-regeneration, as previously shown in conventional BAC filters [19]. At the time of the last sampling for this investigation, BODAC filters have been in operation for 11 years without *ex-situ* regeneration or carbon replacement [2,13], exceeding the typical carbon service life in BAC systems, which ranges from six months to five years depending on the organic loading rate [17, 20,21]. This average service life is mainly for BAC used in drinking water treatment plants, where lower organic loading rate, but stricter regulations apply compared to wastewater reclamation plants [1]. The extended carbon life, together with the efficient removal of biofouling precursors and OMPs, makes the BODAC process attractive not only in the context of UPW production, but also in other wastewater treatment and drinking water production applications.

For this reason, in this work, we investigated the performances of the BODAC filters for 2 years, focusing on the granules' physical and chemical characteristics, biofilm characterization, and the process performances in terms of organics, nutrients, and OMPs removal from wastewater secondary effluent, with the aim to evaluate holistically this unique full-scale scenario. This is the first study presenting a multidisciplinary and comprehensive insight of the BODAC filters, laying the foundation for a deeper understanding of the process for its application as an innovative water treatment approach.

2. Materials and methods

2.1. BODAC filters operation line

The UPW factory, where BODAC filters are in operation (Fig. 1), receives water from the secondary effluent from the nearby WWTP in Emmen, NL. The treatments in the WWTP consists of grit screening, sand removal, pre-settling tank, anaerobic tank, anoxic treatment (de-nitrification), oxic lagoons, and finally secondary clarifier. The secondary effluent then enters the UPW factory and passes first through a drum sieve (1 mm) and then a sub-immerged hollow fiber UF (pore size 0.04 μm), operated at a net flux 28 L m^{-2} h^{-1}. The membranes are backflushed every 6 min and the concentrate is drained twice a day.

The BODAC full-scale setup is comprised of 2 consecutive filters, BODAC 1 and 2 (Fig. 1). The influent of BODAC 1 comprised UF permeate of the previous step, while BODAC 2 influent consisted of the effluent of BODAC 1. The empty bed contact time (EBCT) of BODAC 1 and 2 are 16 and 32 min, respectively [13]. The filtration rate through the BODAC 1 and 2 filters are 10 and 5 m h^{-1}, respectively, and both filters were operated aerobically by regular dosing of pure oxygen at their influent [13]. During the monitoring period, the oxygen concentrations in the influent and effluent of BODAC 1 were 10–23 mg L^{-1} and 7–9 mg L^{-1}, respectively. The oxygen concentrations in the influent and

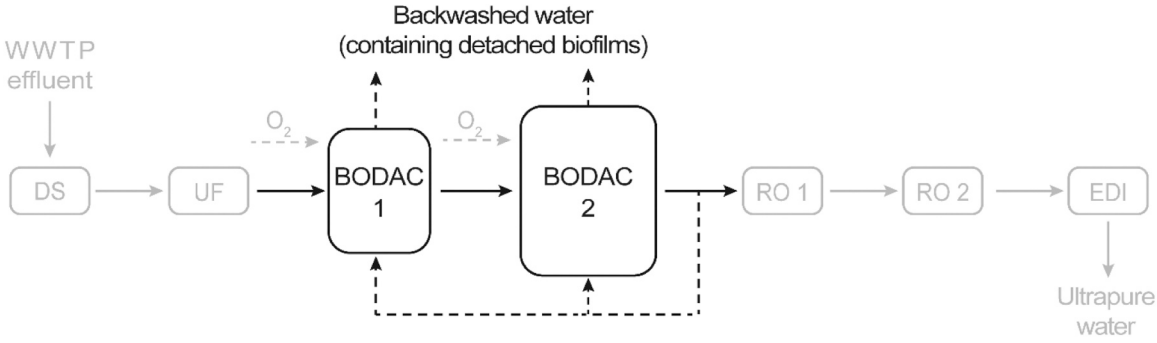

Fig. 1. Schematic overview of the water treatment line at Ultrapure water (UPW) factory, located in Emmen (NL). DS: Drum sieve, UF: Ultrafiltration, BODAC: Biological oxygen-dosed activated carbon, RO: Reverse osmosis, EDI: Electrodeionization, and WWTP: Wastewater treatment plant.

effluent BODAC 2 were 10–13 mg L^{-1}, and 5–8 mg L^{-1}, respectively. The amount of oxygen dosed was adjusted automatically via feedback control instrument based on the oxygen concentration in the BODAC effluent (i.e., around 6–8 mg L^{-1}). A higher oxygen concentration was dosed when a higher ammonia concentration was detected in the influent [22].

Periodical backwashing with air and water was applied on both BODAC filters depending on season or the volume of treated water to decrease pressure build-up due to the accumulation of (bio)solids and avoid excess biofilm growth, without detrimental effects on performances [13]. During the sampling period, backwashing was set based on the volume of water treated. In summer, the backwashing was set every 36×10^3 m^3 of water treated, corresponding to a frequency of 2 days for BODAC 1 and 11 days for BODAC 2. In winter, every 55×10^3 m^3 of water treated, backwashing was set every 3 days for BODAC 1 and every 17 days for BODAC 2. Maximum differential pressure of both filters may not exceed 2.5 mH_2O (normally not achieved prior to backwashing). The water used for backwashing was the effluent of BODAC 2.

2.2. Sampling campaign

A two-year sampling campaign was started from September 2019 until September 2021. The interval between each sampling date was three months, for a total of nine sampling sessions. Granule samples (100 g wet weight) were obtained before and after backwashing from the top of the BODAC filters, and these samples will be referred to as whole (WG) and backwashed granules (BG), respectively. Backwash water samples (1 L) containing detached biofilms were also collected from the top of the filters within the first five minutes after the backwashing started. These samples will be referred to as detached biofilms (DB) samples. Water samples (500 mL), including UF permeate, BODAC 1 effluent, and BODAC 2 effluent, were collected from dedicated sampling ports. All samples were collected in acid-washed LDPE bottles, transported to the lab in a cooling box, and stored in the fridge (4 $\pm$ 2 °C). Both water and DB samples were analyzed within 48 h for chemical analyses and microscopy. Granule samples used for molecular analysis were stored at –20 °C until further processing.

2.3. Granule samples characterization

WG and BG samples from BODAC 1 and 2 were analyzed for their morphological, textural, and chemical characteristics. The virgin granular activated carbon (VGAC) used in the plant, Norit 830P (Cabot, NL), was used as baseline comparison.

2.3.1. Brunauer-Emmet-Teller (BET) analysis

The surface area and porosity of granules (0.5 g for each measurement) were analyzed via BET following the protocol described previously [23], with initial degassing carried out at 105 °C for ~18 h. BET-specific surface area (BET_{SSA}) was determined using the BET model [24]. The non-linear density functional theory (NLDFT) was also applied to determine pore area, pore volume, and pore size distribution [25]. A two-way ANOVA was performed to analyze the effect of different sampling years and backwashing on surface area and porosity of granule samples from BODAC 1 or 2.

2.3.2. Scanning electron microscopy (SEM) and energy dispersive X-ray spectroscopy (EDX)

SEM sample preparation was carried out following the protocol described elsewhere [26], with fixation in 2.5 % glutaraldehyde and drying at 55 °C. Dried 5 granules for each type of sample were coated with gold and observed with SEM (JEOL-6480LV) at an operating voltage of 6 kV. The images were processed using JEOL SEM Control User Interface software (version 7.07). Identification and quantification of relevant chemical elements on 5 granules surface for each type of sample were carried out with energy dispersive X-ray detector x-act SSD-EDX (Oxford Instruments, UK) coupled with the SEM imaging at an acceleration voltage of 15 kV. The percentage of individual elements (aluminum (Al), calcium (Ca), carbon (C), copper (Cu), iron (Fe), magnesium (Mg), manganese (Mn), oxygen (O), phosphorus (P), potassium (K), silicon (Si), sodium (Na), sulfur (S), and zinc (Zn)) were calculated using AZtecOne (version 2.2) (Oxford Instruments, UK).

2.3.3. Inductively coupled plasma optical emission spectroscopy (ICP-OES)

Elemental analysis of the WG and BG samples was carried out using microwave-assisted acid digestion and ICP-OES. The elements measured were Al, Ca, Fe, K, Mg, Mn, Na, and Zn. The samples were dried at 105 °C prior to the analysis. Around 0.5 g dry weight of granules were put in a Teflon tube with 10 mL 69 % HNO_3. The acidified samples were liquefied under pressure (100 bar) for 1 h at 200 °C using the Ethos Easy Microwave digestion platform (Milestone Srl, IT). The digested samples were diluted to 2 % HNO_3 and 2.5 mL of the diluted sample was analyzed with an Optima 5300 DV ICP-OES (Perkin Elmer, US) with argon as the carrier gas. An internal standard of yttrium (Y) (Fluka, CH) was used. The whole analysis was conducted thrice for each type of sample (WG and BG).

2.3.4. Extracellular polymeric substances (EPS) staining and microscopy

EPS staining on ~100 µL of DB samples was carried out by applying 20 µL of either 0.1 % crystal violet (targeting the EPS macromolecules) [27] or 0.01 % alcian blue (targeting the acidic polysaccharides portion) [28]. Both stained and unstained samples were observed under a DM750 microscope (Leica, DE). The microscopy images were acquired using Leica LAS-X (version 4.12) software. The procedure was applied on 5 replicates per sample.

2.3.5. Microbial community analysis

WG samples from BODAC 1 and 2 were used for microbial community analysis based on 16S rRNA gene amplicon sequencing (NGS) analysis. Before DNA extraction, granules were washed with PBS (1x, pH 8.0). The DNA extraction was carried out with the FastDNA™ Spin kit for soil (MP Biomedicals, US) following the manufacturer's instructions. The extracted DNA was quantified using fluorescence spectroscopy (QuantiFluor dsDNA system and Quantus™ Fluorometer (Promega, US)). The V4-V5 region of the 16S rRNA gene of bacteria and archaea was amplified using PCR primers 515F [29] and 926R [30]. Amplicon sequencing was performed at MrDNAlab (Shallowater, US) on a MiSeq (Illumina, US) with 2 × 300 bp (V3) paired-end sequencing. Sequence data were processed for quality check with QIIME2 (v. 2019.10) [31], where DADA2 [32] was used for error-correction and inference of exact amplicon sequence variants (ASVs). For the taxonomic classification of ASVs, reference sequences of SILVA v.138 database were used [33]. Sequencing data were deposited in the European Nucleotide Archive under the project number PRJEB60068.

2.4. Analysis of water samples

2.4.1. Organics, inorganics, and ions determination

To determine the organic and inorganic content in both total and soluble fractions of water samples, chemical oxygen demand (COD), total nitrogen (TN), total and dissolved organic carbon (TOC and DOC, respectively), and proteins measurement were carried out. The soluble fraction was obtained by filtering samples with a 0.45 µm PFTE filter. COD and TN were determined using Hach Lange cuvette tests (Hach Lange, US): LCK 1414 or LCK 314 for COD and LCK 138 for TN, following the manufacturer's instructions. The sample volume required for each replicate measurement for COD and TN was 2 and 1.3mL, respectively. TOC – DOC were measured simultaneously using a Shimadzu TOC-L (Shimadzu, JP) with injection volume of 100 µL. Proteins measurement was carried out using Bicinchoninic acid (BCA) protein assay kit (ThermoScientific, US) with bovine serum albumin as standard. Cations and anions were determined in the soluble fraction of the water

samples. Cations (NH_4^+, Ca^{2+}, Na^+, K^+, and Mg^{2+}) were measured with ion chromatography (IC) (Compact IC Flex 881 and Compact IC Flex 930 (Metrohm AG, CH)) equipped with a Metrosep C4 – 150/4.0 mm column (Metrohm AG) and 3 mM nitric acid as the mobile phase. Anions (Cl^-, SO_4^{2-}, NO_2^-, NO_3^-, and PO_4^{3-}) were measured with Ion Chromatograph Compact IC 761 (Metrohm AG) using a Metrosep A Supp 5, 150/4.0 mm column. The first mobile phase consisted of 3.2 mM sodium carbonate, 1 mM sodium bicarbonate, and 1 % (v/v) acetone. The second mobile phase consisted of 0.5 mM orthophosphoric acid and 1 % (v/v) acetone. The injection volumes of the sample for cation and anion measurement were 100 µL and 20 µL, respectively. Other trace metals (Al, Mn, Fe, and Zn) were measured on unfiltered samples using ICP-OES after addition of HNO_3 (2 % final concentration in solution). Calibration curves for IC and ICP-OES were determined as described in Supplementary Information.

2.4.2. OMPs analysis via liquid chromatography mass-spectrometry tandem mass-spectrometry (LC–MS/MS)

The concentration of thirteen OMPs of interest in the process water samples was monitored during the 2-year period, namely: atenolol (ATE), carbamazepine (CAR), clarithromycin (CLA), diclofenac (DIC), gabapentin (GAB), hydrochlorothiazide (HYD), irbesartan (IRB), lidocaine (LID), metoprolol (MET), propranolol (PRO), sotalol (SOT), and trimethoprim (TRI) and benzotriazole (BEN). The OMPs measurement was carried out using LC-MS/MS 6420 Triple Quad Mass Spectrometer (Agilent, US) equipped with a UHPLC guard Zorbax Eclipse Plus C18 1.8 µm, 2.1 × 5 mm as pre-column and Zorbax Eclipse Plus C18 RRHD 1.8 µm, 50 × 2.1 mm as the column (Agilent). A gradient of 10 mM ammonia, 10.4 mM formic acid, and 0.04 mM oxalic acid eluent A, and acetonitrile as eluent B was used. The sample volume injected was 5 µL. The OMP concentration was determined by using a standard calibration curve for each OMP, within concentration range of 0–67.2 µg L^{-1}. Internal standards of atenolol-D7 (18 µg L^{-1}), ciprofloxacin-D8 (32 µg L^{-1}), dihydrocarbamazepine (30 µg L^{-1}), fenoprofen (37 µg L^{-1}), and trimethoprim-D9 (32 µg L^{-1}) were used. Detailed information regarding physicochemical property, ionization method, precursor and product ions, time segment, and detection limit for each OMP from the analysis are provided in Tables S1, S2, and S3 of Supplementary Information.

3. Results and discussion

3.1. BODAC granules morphology and textural properties

As expected from the granule samples' age (between 9 and 11 years), BET_{SSA} of BODAC 1 and 2 WG sampled between 2019 and 2021 was reduced by around 70 % compared to VGAC (Fig. 2A), indicating that less surface area was available for adsorption in aged granules. The BET_{SSA} of aged granules differed significantly among the sampling years for BODAC 1 ($F_{2,12} = 7.73$, $p = 0.007$) and BODAC 2 ($F_{2,11} = 29.65$, $p < 0.001$) (Fig. 2A), and fluctuated between 275 and 350 m^2/g in BODAC 1 and between 110 and 270 m^2/g in BODAC 2 during the monitoring period, i.e., showing a relative stability within this range. Additionally, while a minor positive influence of backwashing was observed for BET_{SSA} of BODAC 1 ($F_{1,12} = 32.09$, $p < 0.001$), backwashing was unable to restore BET_{SSA} to a level comparable to VGAC (Fig. 2A). The WG surface characteristics were investigated via SEM analysis by comparing with the VGAC (Fig. S1A and B) with BODAC 1 and 2 samples (Fig. 2B), where thick biofilms and different cells were visible, together with inorganic deposits. After backwashing, substantial biofilms and inorganic deposits were still visible on both BODAC 1 and 2 granules, but to a lesser extent than on WGs (Fig. S1C and D). Biofilms growing on top of the WGs were further characterized from DB samples using specific staining for EPS, showing a complex matrix rich in acidic polysaccharides with some black inorganic particles (Fig. 2C). The inorganic deposits visualized via SEM and their concentrations were quantified via ICP-OES and SEM-EDX for both WG and BG for BODAC 1 and 2, highlighting the accumulation of different metals (Fig. 3 and Table S4 and S5).

The ICP-OES analysis (Fig. 3A) showed that manganese (Mn) was accumulated on BODAC 1 WGs (Fig. 3A, in grey), while its amount on BGs was significantly lower ($p < 0.05$) (Fig. 3A, in white). This suggested that Mn was included within biofilms, which was supported by optical microscopy analysis (Fig. 2C, black deposits), and that Mn was thus mostly removed during backwashing. The decrease of Mn after backwashing was also observed based on EDX analysis (Fig. 3B). A lower accumulation of Mn was observed on BODAC 2 WGs ($p < 0.05$), which was also removed during backwashing (Fig. 3A). Mn removal in BAC systems is likely connected with the activity of manganese oxidizing bacteria (MOB) which convert Mn (II) to insoluble manganese oxides (MnOx) on the granules' surface [34]. In such systems, most of the precipitated MnOx will be then washed out together with the biofilm during backwashing [35].

Elemental analysis via ICP-OES also indicated an accumulation of Ca and Fe, but likely due to adsorption into the BODAC granules since backwashing hardly removed them from the samples (Fig. 3A). Accumulation of metals, e.g., Ca and Fe, on GAC have been frequently observed [36], and backwashing did not lead to the removal of these metals from BAC [37]. Ca was commonly deposited as calcium carbonate ($CaCO_3$) [36] or as a complex with humic substances [38]. Deposition of $CaCO_3$ or Ca-humics complexes in the pores of GAC might contribute to their lower BET_{SSA} compared to VGAC (Fig. 2A). EDX analysis showed a small accumulation of Ca and Fe on the surface of the WG and BG samples (Fig. 3B), and due to the limited penetration depth of this technique (~ 5–10 µm, depending on the power of the primary electron beam), this result further suggested such accumulation took place in the pores rather than on the outermost surface.

3.2. Process performance of BODAC filters

3.2.1. Soluble organic compounds were still removed in BODAC filters after 11 years of operation

The organic content of the BODAC filter influent was constituted by soluble molecules, most of which were identified as proteins (Fig. S2A and B). The DOC to sCOD (DOC:sCOD) ratio in BODAC 1 and 2 influents during the monitoring period typically ranged from 0.4 to 0.5:1, except in December 2019 and March 2020, where the DOC:sCOD ratio was 1:1. During the 2 years of monitoring, around 10–45 % of the organics were removed by BODAC 1 and 2 (Fig. 4). Concentrations and removal of both sCOD and soluble proteins showed almost identical patterns, suggesting that the organic materials removed in the BODAC filters primarily consisted of proteins (Fig. S2). BAC systems were reported to perform better at removing proteins from water compared to GAC due to biodegradation [4]. As often detected in secondary wastewater effluents, the residual sCOD can be composed of non-biodegradable soluble organic matter, which could not be further oxidized by the BODAC biofilms [39]. Among these, humic acids often constitute the majority of the organic fraction in secondary effluents, which can cause membrane fouling when not removed from the water stream [40].

At the start of the BODAC filters operation (in 2011), the COD rapidly decreased from 99 % to 50 % in the first 100 days of operation, most likely due to adsorption. In the period between 100 to 200 days, the removal decreased from 50 % to 30 %, and after 200 days of operation, the removal fluctuated between 10 % and 30 % [13], suggesting the switch from adsorption to biodegradation as dominant removal mechanism. These results are in line with the three phases of organics removal described for BAC processes: (i) adsorption only; (ii) transition from adsorption to biodegradation; (iii) stationary phase, when oxidative biodegradation by the biofilms prevails and organics removal range is 10–40 % [17]. Therefore, the current BODAC filters had reached their stationary phase but were still removing biofouling precursors and no significant fouling issues were reported [13], and were actively removing OMPs for 11 years. The BODAC service life was 2–3 times

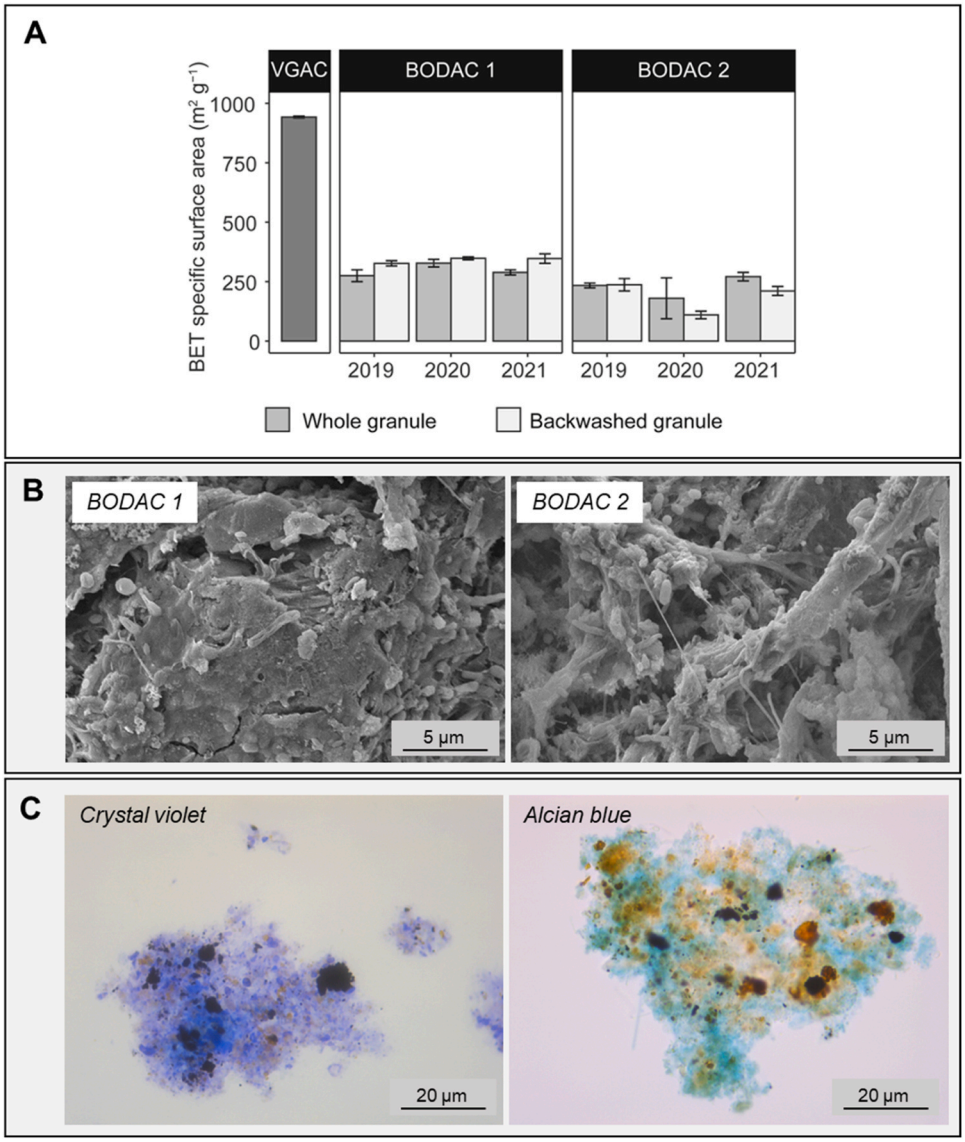

Fig. 2. Analyses of BODAC aged granules. A. Comparison of Brunauer-Emmet-Teller (BET) specific surface area of Virgin Granular Activated Carbon (VGAC), whole granules, and backwashed granules samples from BODAC 1 and 2 (n = 3, error bars represent standard deviation); B. Representative image of the surface morphology of BODAC whole granule samples observed with Scanning Electron Microscopy (SEM); C. Representative micrographs of the biofilm's matrix growing on BODAC granules, collected from backwash water, after EPS staining of the whole matrix (crystal violet), and the acidic polysaccharides fraction (alcian blue).

longer compared to other BAC filters, which no longer produced the desired water quality after 3–5 years of operation and required regeneration [41]. Backwashing led to a lower removal of organic compounds in BODAC 1 (Fig. S3), but the total removal after treatment using BODAC 1 and 2 remained the same. Previously, other researchers also observed lower degradation of organics after backwashing due to the removal of the loosely-bound fraction of the biofilm, but the removal capacity could recover over time as the biofilm also recovered [42].

3.2.2. *Nitrification and manganese removal consistently took place in BODAC filters*

In the BODAC influent, the total nitrogen was comprised of different species, namely ammonium (NH_4^+), nitrite (NO_2^-), nitrate (NO_3^-), and organic nitrogen (Fig. 5). After treatment in BODAC 1 and 2, the total nitrogen remained the same as in the influent, i.e., no net uptake of nitrogen, but all NH_4^+ and NO_2^- were converted to NO_3^-, showing complete nitrification of the 2 years oxidizable nitrogen species in BODAC 1 (Fig. 5). Interestingly, further nitrification took place in BODAC 2, possibly due to in-situ conversion of organic nitrogen, i.e., proteins to ammonium, which is then used as a substrate in the nitrification process. Regardless of its initial concentration in the BODAC 1 influent, NH_4^+ was fully oxidized in this filter. The average NH_4^+ in the BODAC 1 influent was around 2–5 mg L^{-1}, and theoretically, it required 9.2–25 mg L^{-1} oxygen to fully oxidize it (4.57 g O_2/g NH_4-N) [43]. This would then suggest that the oxygen dosing could have been beneficial for the nitrification process in the BODAC filter. Biological nitrification is commonly observed in BAC filters [44,45]. It comprises of three reactions: (i) conversion of NH_4^+ to hydroxylamine catalyzed by ammonia monooxygenase (AMO); (ii) conversion of hydroxylamine to NO_2^- by hydroxylamine oxidase (HAO); (iii) conversion of NO_2^- to NO_3^- by nitrate oxidoreductase (NXR) [46]. Details of biological nitrification reactions are schematized in Fig. S4.

As observed for NH_4^+ and NO_2^-, Mn was also consistently removed completely from the influent after treatment with BODAC filters, regardless of the initial concentration and season (Table 1). In most cases analyzed, almost complete removal of Mn took place already in BODAC 1, with very low concentrations reaching BODAC 2. The removal of Mn from the influent water by BODAC 1 connects with the high Mn retention observed within these granules (Fig. 3, Tables S4 and S5). A lower removal of Mn in BODAC 1 was observed in December 2019 and 2020 (Table 1), which could be due to lower temperatures, especially if the Mn removal was due to biological Mn oxidation [47].

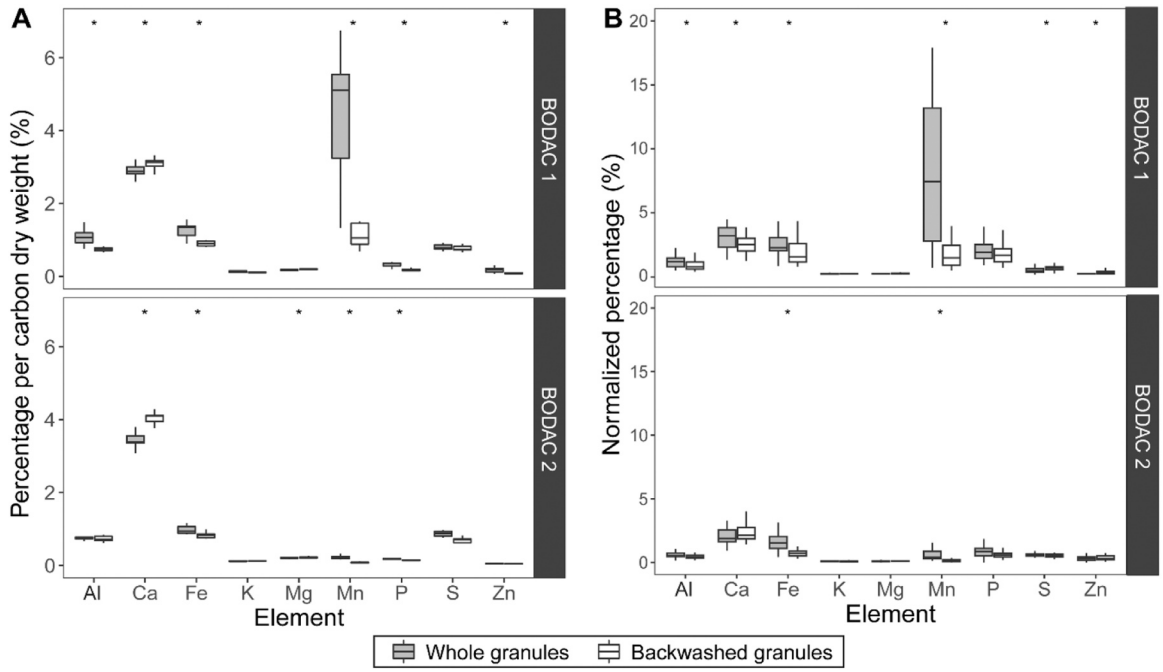

Fig. 3. Element concentrations in BODAC 1 and 2 granules during 2 years of sampling. Analyses were performed via: (A) Microwave assisted digestion and ICP-OES (n = 18, error bars represent uncertainty or variation); (B) EDX analysis of the granules surface (n = 70). The middle line in the box represents the median, while the bottom line and top lines of the box represent the 1st and the 3rd quartile. The whiskers (vertical lines) extend from the ends of the box to the minimum and maximum values based on 1.5 times the interquartile range. The asterisks symbol represents statistically significant differences between whole (WG) and backwashed granules (BG) where *=$p < 0.05$ indicated by ANOVA tests (the summary statistics are presented in Table S6 and S7).

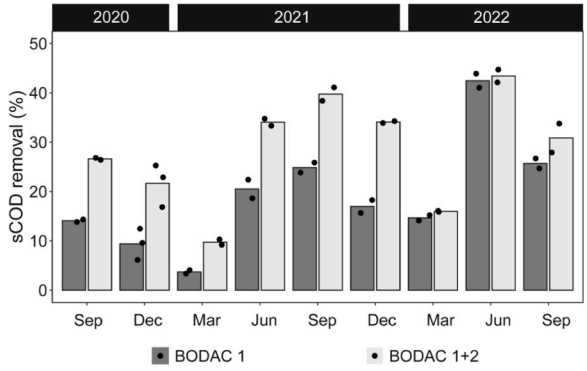

Fig. 4. Removal of soluble chemical oxygen demand (sCOD) after treatment of the influent water with BODAC 1 only and BODAC 1 + 2 during the 2-year monitoring period (n = 2–3, all data points were plotted using dot markers, bar graphs show the mean average).

Among the other cations analyzed, Fe concentration was also reduced from the water after BODAC treatment (35–67 %, Table 1). Fe release from BODAC was also observed in some samples (Table 1), indicating that reversible adsorption of Fe was likely the main removal mechanism. A net removal of Ca from the effluent was not observed (Table 1), thus the detection of this cation within the granules (Table S4) and on the surface (Table S5) suggested that such accumulation was due to adsorption and precipitation phenomena into the pores in past years of BODAC operation. Ca commonly accumulates on GAC, and when it is chelated by the organic matter, it is drawn into the pores, decreasing the pore size and adsorption capacity [38]. Lee and colleagues [36] observed that, during the long-term operation of BAC, such accumulation was still taking place after 3.5 years of operation. Due to the exceptionally long service life of BODAC filters, we can speculate that such Ca accumulation reached a saturation, hampering the Ca removal from the influent water but not significantly affecting the granules' biodegradation performances.

3.2.3. *Most OMPs of interest were removed to a very high extent in BODAC filters*

The influent of BODAC filter 1 contained OMPs originating from the secondary effluent of a WWTP. The removal of thirteen OMPs within BODAC filters was analyzed for two years (Table 2), which varied in time depending mainly on the fluctuating influent concentrations (Table S8). We categorized the OMPs removal as well (>70 %), moderately (30–70 %), and poorly removed (<30 %) based on their median removal (Table 2). Among all OMPs of interest, ATE, HYD, LID, MET, SOT, and TRI were well removed (>70 %) in BODAC 1 and 2 in more than six of the time points analyzed (Table 2). CLA, DIC, IRB, and PRO were moderately removed in BODAC 1. Further removal of CLA, DIC, and IRB took place in BODAC 2, but not for PRO. As a result, the total removal (BODAC 1 + 2) of CLA and DIC was >70 %, yet for GAB, the total removal remained <70 %. GAB, a highly water-soluble and hydrophilic compound, was removed variably along the sampling dates (12–92 %), and its removal was not affected by its initial concentration (Table S8) or water temperature (Table 2), but could be possibly related to the presence of specific heterotrophic microorganisms able to degrade it [48]. BEN and CAR were either poorly removed (<30 %) or desorbed to the water (Table 2). BODAC 1 contributed to at least half of the total removal (%) of the OMPs in the series of BODAC filters (1 + 2). Only IRB, a low-water soluble and highly hydrophobic compound (Table S2), was removed better in BODAC 2. The IRB removal was expected since the EBCT in BODAC 2 was higher than in BODAC 1, facilitating its adsorption to carbon granules. Nevertheless, BODAC 2 performed as a polishing filter and contributed to the overall removal of OMPs. The water temperature influenced the HYD and MET removal in BODAC 1 (Table 2), with decreased removal efficiencies observed at temperatures lower than 13 °C in comparison to other samples. This tendency was not observed for other OMPs, for which removal in BODAC 1 could be affected by their initial concentrations or other factors. No particular removal pattern was observed for OMPs with different physicochemical

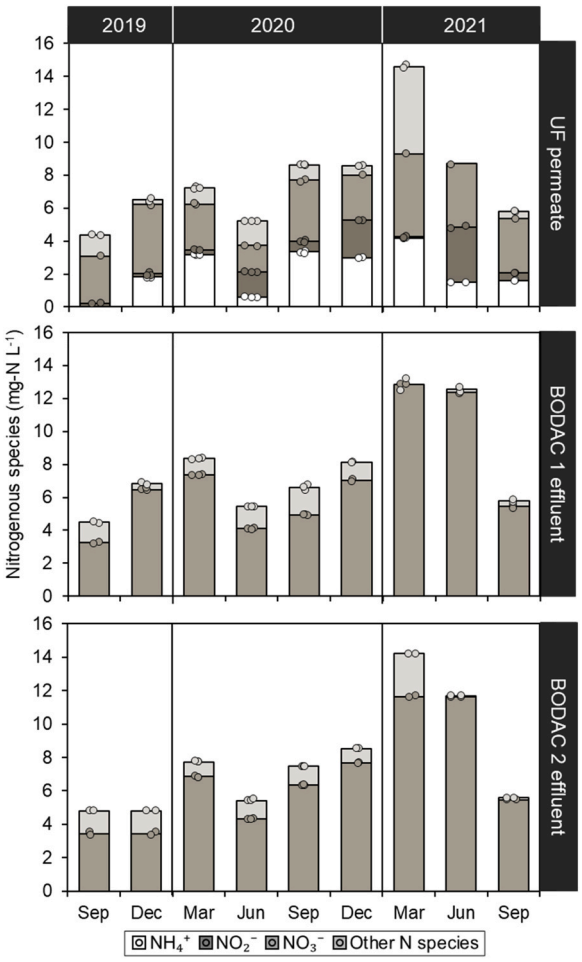

Fig. 5. Profile of nitrogenous species in the influents and effluents of BODAC 1 and 2 filters during the 2-year monitoring period (n = 2 or n = 3, all data points were plotted using dot marker, bar graphs show the mean average).

characteristics (Table S1) which was also reported in other BAC filters [49]. This is plausible since the carbon pores and surfaces were covered with biofilm and inorganics depositions, as mentioned in Section 3.1. The presence of inorganic deposits and microorganisms made the surface of the carbon much more heterogenous (Figs. 2 and 3), making the removal of OMPs on the BODAC granules more challenging to be predicted by the hydrophobicity and/or charge of OMPs.

Some of the OMPs removal in BODAC filters, especially BODAC 1 was higher than previously reported in other engineered systems. For example, HYD removal was around 70 % [50], while in BODAC 1, >90 % removal of HYD could be achieved. This could be due the dosing of pure oxygen into BODAC filters that helps maintaining aerobic conditions favoring biodegradation/biotransformation [48] and could boost oxidation reactions [51]. Moreover, the presence of an adapted microbial community capable of degrading a broad range of OMP is equally important [50]. In BODAC 1, high nitrification and Mn removal activities are expected from results presented in the previous sections. Past research showed a possible role for nitrification enzymes (AMO, HAO, and NXR) in the indirect biodegradation/biotransformation of OMPs [48,50,52]. Research was particularly focused on the role of AMO, which is known to be able to degrade aromatic compounds with similar structures as some OMPs [48,52]. In the same way, the biogenic manganese oxide (MnOx) produced by MOB can contribute to OMPs removal by adsorption or by catalysis, often leading to their complete removal [53,54]. Besides these indirect mechanisms, direct degradation of OMPs can be catalyzed by several specific bacterial enzymes, as discussed in the following section.

3.3. *Putative nitrifying and manganese oxidizing bacteria were detected in high relative abundance on BODAC granules*

Microbial community analysis was carried out to determine the possible microbial protagonists driving the processes nitrification and Mn(II) oxidation. DNA extracted from WGs samples from BODAC 1 and 2 was used for amplification and sequencing of 16S rRNA gene fragments, and the results are shown in Fig. 6. For both BODAC 1 and 2 filters, part of the microbial community remained unclassified, thus limiting the possibility to connect the entire community with putative functions in the BODAC filters. However, most of the dominant community members identified are related to either nitrogen removal or Mn (II) oxidation, supporting the hypothesis that biology drives the main process dynamics observed in BODAC filters (see previous sections).

Microbes catalyzing nitrogen removal were dominant in both BODAC 1 and 2. In BODAC 1, the dominant genus was *Nitrospira,* nitrite-oxidizing bacteria (NOB) that are considered as the main drivers of NO_2^- oxidation in several natural and anthropogenic environments including WWTPs [55]. In WWTPs, NOB typically cooperate with ammonia oxidizing bacteria (AOB) such as *Nitrosomonas* (2.8 % relative abundance in BODAC 1, Fig. 6) to oxidize NH_4^+ to NO_3 via NO_2^- [56]. A relatively low NH_4^+ content in the influent and a continuous flow, limiting NO_2^- production, usually favors the growth of *Nitrospira* in these

Table 1
Metal removal (%) in BODAC 1 only or BODAC 1 and 2 during the 2-year monitoring period (n = 2 ± difference of the two data points). Negative values indicate the release/desorption of the metal into the water. Median average (mdn avg) was calculated to estimate the overall removal trends.

Metal	BODAC Filter	Removal (%)									
		Sep-19	Dec-19	Mar-20	Jun-20	Sep-20	Dec-20	Mar-21	Jun-21	Sep-21	Mdn avg
Al	1	66 ± 8	15 ± 5	51 ± 7	45 ± 7	57	8 ± 1	25 ± 2	n.m.	95	48 ± 29
	1 + 2	67 ± 1	52 ± 5	60 ± 5	89 ± 1	74 ± 3	47 ± 1	43 ± 1	n.m.	95	63 ± 19
Ca	1	5 ± 3	3 ± 1	4 ± 1	8 ± 2	3 ± 2	7 ± 1	1 ± 1	–78 ± 1	4 ± 1	4 ± 27
	1 + 2	1	3 ± 1	9 ± 1	12	2 ± 1	11	2 ± 1	–75 ± 3	6 ± 1	3 ± 27
Fe	1	31 ± 1	–16 ± 5	15 ± 9	24 ± 4	52	–4	20	–9 ± 6	37 ± 3	20 ± 23
	1 + 2	40 ± 2	35 ± 5	37 ± 3	58 ± 1	67	50	41 ± 1	53 ± 1	41 ± 1	41 ± 11
K	1	9 ± 4	8 ± 1	0 ± 4	2 ± 3	5 ± 1	3 ± 3	5 ± 1	–68 ± 1	3	3 ± 25
	1 + 2	9 ± 1	9 ± 1	4 ± 2	6	4 ± 1	3 ± 1	6 ± 1	–71 ± 1	4	3 ± 27
Mg	1	5 ± 5	3 ± 2	2 ± 1	5 ± 2	4 ± 1	5 ± 1	2	–70 ± 2	0	3 ± 24
	1 + 2	–2	2 ± 1	16 ± 1	15 ± 3	6 ± 1	15 ± 1	3 ± 1	–73 ± 2	2 ± 1	4 ± 26
Mn	1	99	61 ± 2	96	88 ± 1	99	64 ± 1	91	86 ± 1	98	91 ± 14
	1 + 2	99	99	99	99	99	99	98	100	99	99 ± 0
Na	1	4 ± 4	5 ± 1	0	0 ± 2	4	0	0	–75 ± 1	2 ± 1	0 ± 26
	1 + 2	2	5	2 ± 1	1 ± 1	3	–1	1	–75 ± 2	2	2 ± 26
Zn	1	30 ± 1	38 ± 1	11 ± 4	–63 ± 12	–51 ± 7	25	21	47 ± 1	49	25 ± 41
	1 + 2	22 ± 1	–53 ± 6	3 ± 3	–248 ± 51	–192 ± 10	4 ± 3	17 ± 1	–5	–88 ± 15	–5 ± 98

Table 2
Organic micropollutants (OMPs) removal after treatment of influent water with Biological Oxygen Dosed Activated Carbon (BODAC) filters (n = 2 ± difference of the two data points). Removal (%) was calculated by the difference of influent and effluent concentration, and when the concentration was lower than the limit of detection (LOD), it was corrected with LOD$\sqrt{2}$. n.m: not measured. Median average (mdn avg) was calculated to estimate the overall removal trends.

OMP	BODAC Filter	Removal (%)									
		Sep-19	Dec-19	Mar-20	Jun-20	Sep-20	Dec-20	Mar-21	Jun-21	Sep-21	Mdn avg
Atenolol (ATE)	1	40	71 ± 4	73 ± 5	82 ± 7	86 ± 2	76 ± 3	50 ± 3	23 ± 23	88 ± 4	75 ± 21
	1 + 2	40	71 ± 4	77 ± 3	89	93	92	83	74 ± 5	90	83 ± 13
Benzotriazole (BEN)	1	–14	28 ± 6	18 ± 2	7 ± 2	3 ± 2	30 ± 1	16 ± 2	–210 ± 16	–40 ± 8	8 ± 69
	1 + 2	–7	42 ± 3	24 ± 2	13 ± 3	11 ± 1	38	23 ± 3	–243 ± 30	–68 ± 9	17 ± 83
Carbamazepine (CAR)	1	4	–38 ± 8	1 ± 9	25 ± 2	28 ± 3	20 ± 1	7 ± 3	–68 ± 30	28 ± 6	11 ± 33
	1 + 2	30	–24 ± 14	6 ± 14	39 ± 2	43 ± 2	43 ± 13	22 ± 1	–60 ± 28	40 ± 2	30 ± 35
Clarithromycin (CLA)	1	58	58 ± 12	12 ± 30	43 ± 13	n.m.	56	24 ± 18	n.m.	43	45 ± 23
	1 + 2	78	91 ± 2	75 ± 27	91 ± 1	n.m.	56	60 ± 6	n.m.	43	89 ± 19
Diclofenac (DIC)	1	79	77 ± 7	27 ± 8	2 ± 17	72 ± 12	-12	52 ± 4	76	88 ± 3	64 ± 37
	1 + 2	89	87 ± 2	82 ± 2	76 ± 4	93 ± 1	50	94	76	88 ± 3	88 ± 11
Gabapentin (GAB)	1	51	41 ± 5	5 ± 2	33 ± 3	6 ± 5	36 ± 28	10 ± 1	98 ± 1	52 ± 2	34 ± 28
	1 + 2	67	72 ± 4	12 ± 4	55 ± 1	12 ± 7	32 ± 1	52 ± 1	92 ± 1	64	54 ± 28
Hydrochlorothiazide (HYD)	1	n.m.	n.m.	75 ± 1	90 ± 3	92 ± 1	86	73 ± 6	95 ± 1	98	91 ± 10
	1 + 2	n.m.	n.m.	92	97	98 ± 1	98	98	95 ± 1	98	98 ± 3
Irbesartan (IRB)	1	23	33 ± 5	8 ± 3	17 ± 2	34 ± 2	18 ± 1	12 ± 2	94	36 ± 1	23 ± 24
	1 + 2	85	79 ± 3	54 ± 1	86	89 ± 1	78 ± 3	64 ± 1	94	95	85 ± 14
Lidocaine (LID)	1	73	73 ± 0	90 ± 1	82 ± 1	70 ± 1	66 ± 9	76 ± 1	56	78 ± 1	73 ± 10
	1 + 2	73	73 ± 0	90 ± 1	82 ± 1	70 ± 1	66 ± 9	76 ± 1	56	78 ± 1	73 ± 10
Metoprolol (MET)	1	87	79 ± 4	66 ± 5	84 ± 2	86 ± 2	79 ± 1	56 ± 4	55	88	80 ± 12
	1 + 2	96	97 ± 0	96	98	98	98 ± 1	88	86 ± 1	98	97 ± 4
Propranolol (PRO)	1	n.m.	33	n.m.	66 ± 3	62 ± 3	69	69 ± 3	53 ± 4	66 ± 8	64 ± 10
	1 + 2	n.m.	33	n.m.	66 ± 3	62 ± 3	69	69 ± 3	53 ± 4	66 ± 8	64 ± 10
Sotalol (SOT)	1	71	82 ± 2	87 ± 2	96	96	96 ± 1	86 ± 1	91	96	91 ± 7
	1 + 2	71	75 ± 12	87 ± 2	96	96	96 ± 1	96	91	96	96 ± 9
Trimethoprim (TRI)	1	n.m.	80 ± 18	91 ± 1	94 ± 1	91 ± 2	70 ± 4	82 ± 1	n.m.	n.m.	91 ± 10
	1 + 2	n.m.	80 ± 18	91 ± 1	94 ± 1	91 ± 2	70 ± 4	82 ± 1	n.m.	n.m.	91 ± 10
Water temperature (°C)		19	11	9	18	20	13	9	17	20	17 ± 5

systems [57], similar to what was observed in BODAC 1. In BODAC 2, among the dominant groups, we identified members of the family *Nitrosomonadaceae* (MND1 and IS-44), AOB converting NH_4^+ to NO_2^- [58], and again *Nitrospira* to exert the NOB function (Fig. 6). These results are in line with the analysis of nitrogen species present in BODAC 1 and 2 (Fig. 5). Interestingly, many microbial community members identified on BODAC 1 and 2 granules were related to Mn oxidizers.

Pedomicrobium and *Hyphomicrobium* are widely reported in the literature as being able to oxidize soluble Mn(II) to insoluble manganese oxide [59,60] and are connected to the formation of Mn nodules [61]. These bacteria can increase the rate of Mn oxidation to five times that of non-biological Mn oxidation [62]. Other microbial groups detected in BODACs were reported to be likely connected with Mn oxidation, such as *Stenotrophobacter* [63], *Terrimonas* [64], *Burkholderiaceae* [64], *Gammaproteobacteria* PLTA13 [63], or to require Mn for growth, as observed for *Bradyrhizobium* [65] (Fig. 6). A recent study established that a bacterium affiliated with the phylum *Nitrospirae* was capable of Mn(II)-oxidation [66], while *Nitrosomonadaceae* MND1 was found in ferromanganese nodules within caves [67]. Previous research showed that nitrification can create the conditions favoring biological Mn oxidation and that activity of Mn-oxidizing bacteria in mixed cultures can be stimulated by the presence of nitrifiers [68], which are essential in order to eliminate NO_2^- and its negative effects on biological Mn oxidation [68,69]. The simultaneous removal of NH_4^+ and trace metals such as Fe and Mn was achieved in different biotechnological systems [70,71], highlighting the existence of cooperation between these 2 years bacterial groups which can be beneficial for water treatment approaches, as observed in the BODAC filters. Among the groups putatively involved in the direct degradation of OMPs, members of the *Rhizobiales* family, e.g., *Bradyrhizobium* and *Hyphomicrobium* are known to be capable of degrading aromatic compounds and contributing to bioremediation of contaminated soil [72].

4. Connecting the dots: relevance of BODAC process and future perspectives

The purpose of the BODAC concept was to introduce a pre-treatment, together with low-pressure UF, which could improve the removal of (recalcitrant) organic matter and foulants, to reduce the maintenance of RO units included in the production line of ultrapure water (Fig. 1). In the present study, a holistic approach analyzing granules and water samples of BODAC filters was carried out for two years to understand the mechanisms behind the long-term operation of this AC-based biotechnology for 11 years. The carbon service life of is one of its interesting features since it was reported that BAC filter adsorption capacity decreased after 6 years of operation, requiring replacement or regeneration [20]. Aged BODAC granules had a significantly reduced surface area in comparison to VGAC (Fig. 2A), corresponding to a complex surface morphology with biofilms, cells, and inorganic deposits, which did not change even after backwashing (Fig. 2B and Fig. S1). Inorganics were accumulated on the surface (and in the pores) of the granules, such as Ca, Fe, P, Al, and above all Mn (Fig. 3, Table S2 and S1). Mn was always completely removed from the influent water within the BODAC filters (Table 1), likely due to its biological conversion to black, insoluble MnOx included in the biofilm (Fig. 2C). Inorganic accumulation combined with biofilm growth are usually deteriorating BAC performances due to precipitation, pore-clogging, and thus a reduced surface area [36,73].

The conditions imposed in BODAC filters, such as EBCT (16 min for BODAC 1 and 32 min for BODAC 2), pure oxygen dosing (average 16 mg L^{-1}, 55 % dosed in BODAC 1 % and 45 % in BODAC 2), and the frequency of backwashing (once every 2–3 days for BODAC 1 or 11–17 days for BODAC 2) [12], ensure consistent performances. Complete nitrification was always achieved during the process (Fig. 5), the enzymatic activity of the nitrifying bacteria could significantly contribute to the co-metabolism of OMPs [48]. Similarly, Mn oxidation was probably catalyzed by several microbial groups identified in the granules communities (Fig. 6), and the presence of MnOx could be related to

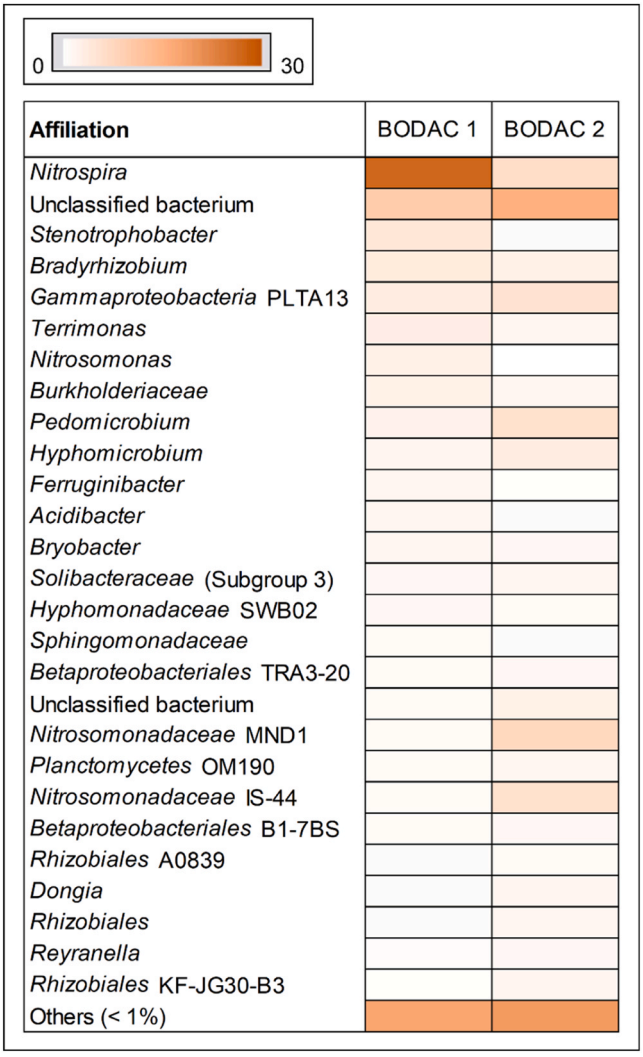

Fig. 6. Relative abundances of dominant bacterial groups (>1 % relative abundance) identified via microbial community analysis using 16S rRNA gene amplicon sequencing of whole granules sampled from BODAC 1 and 2, reported as a percentage (in the range 0–30 %), and their taxonomy classification at the identified level. All amplicon sequence variants <1 % are summed together and presented as Others (n = 3, the percentage value is the mean average).

improved organics and OMPs removal [74]. Since Mn is known to be one of the main causes of irreversible fouling in membrane systems [75], biological Mn removal could contribute to avoiding significant fouling phenomena of RO units. The removal of OMPs by BODAC is an added value towards the production of ultrapure water, also overcoming the limit of OMPs accumulation in the permeate after rejection by the RO membranes [76]. Pure oxygen alone could also contribute to partial oxidation of organics and OMPs and stimulate the oxidation of Mn, both via abiotic and biotic pathways [74]. Most of the processes described were already fully exploited in BODAC 1 (Table 1, Table 2, Fig. 4, Fig. 5), suggesting that a single treatment line could be enough, considering future applications of this biotechnology for water treatment. Future investigations will focus on further characterization of both the abiotic and biotic parameters/processes which all together are keeping the BODAC system long-lasting, active, and stable. In conclusion, this study demonstrated that BODAC filters are a promising bio-based tertiary treatment to further remove foulants and OMPs in WWTP effluent by harnessing the microbiological growth in the filter.

CRediT authorship contribution statement

Olga Bernadet: Conceptualization, Methodology, Validation, Formal analysis, Investigation, Writing – original draft, Writing – review & editing. **Amanda Larasati:** Methodology, Validation, Formal analysis, Investigation, Writing – original draft, Writing – review & editing. **H. Pieter J. van Veelen:** Methodology, Validation, Formal analysis, Data curation, Writing – review & editing. **Gert Jan Willem Euverink:** Conceptualization, Validation, Writing – review & editing, Supervision, Funding acquisition. **Maria Cristina Gagliano:** Conceptualization, Methodology, Validation, Writing – original draft, Writing – review & editing, Supervision, Project administration.

Declaration of Competing Interest

The authors declare that they have no known competing financial interests or personal relationships that could have appeared to influence the work reported in this paper.

Data Availability

Data will be made available on request.

Acknowledgements

This work was supported by the cooperation framework of Wetsus, European Centre of Excellence for Sustainable Water Technology (www.wetsus.eu) and the members of Advanced Water Treatment Theme. Wetsus is co-funded by the Dutch Ministry of Economic Affairs and Ministry of Infrastructure and Environment, the European Union Regional Development Fund, the Province of Fryslan and the Northern Netherlands Provinces. The authors thank Gerrit Veenendaal for his shared knowledge about BODAC, and Bennie Bakker and Eran Amar for their help during the 2-year sampling campaign and for their shared knowledge about BODAC operation. We also thank the analytical team at Wetsus, especially Mieke Kersaan-Haan for her valuable help during LC–MS/MS measurement, Rudmer Bakker for the DNA extractions, and Bert Geurkink for his help during processing of the NGS raw data. We also thank the members of Advanced Water Treatment Theme for the shared knowledge and financial support.

Appendix A. Supporting information

Supplementary data associated with this article can be found in the online version at doi:10.1016/j.jhazmat.2023.131882.

References

[1] Granzoto, M.R., Seabra, I., Malvestiti, J.A., Cristale, J., Dantas, R.F., 2021. Integration of ozone, UV/H2O2 and GAC in a multi-barrier treatment for secondary effluent polishing: reuse parameters and micropollutants removal. Sci Total Environ 759, 143498. https://doi.org/10.1016/j.scitotenv.2020.143498.
[2] G. Veenendaal, D. Kuiper, S. Dost, P. Van der Maas, Ultrapuur water uit RWZI-effluent; bijna 10 jaar ervaring in Emmen, H2O/Waternetwerk. (2019). https://www.h2owaternetwerk.nl/vakartikelen/ultrapuur-water-uit-rwzi-effluent-bijna-10-jaar-ervaring-in-emmen.
[3] Ang, W., Elimelech, M., 2007. Protein (BSA) fouling of reverse osmosis membranes: implications for wastewater reclamation. J Membr Sci 296, 83–92. https://doi.org/10.1016/j.memsci.2007.03.018.
[4] Pramanik, B.K., Roddick, F.A., Fan, L., 2014. Effect of biological activated carbon pre-treatment to control organic fouling in the microfiltration of biologically treated secondary effluent. Water Res 63, 147–157. https://doi.org/10.1016/j.watres.2014.06.014.
[5] Badruzzaman, M., Voutchkov, N., Weinrich, L., Jacangelo, J.G., 2019. Selection of pretreatment technologies for seawater reverse osmosis plants: a review. Desalination 449, 78–91. https://doi.org/10.1016/j.desal.2018.10.006.
[6] Cornelissen, E.R., Harmsen, D.J.H., Blankert, B., Wessels, L.P., van der Meer, W.G. J., 2021. Effect of minimal pre-treatment on reverse osmosis using surface water as a source. Desalination 509, 115056. https://doi.org/10.1016/j.desal.2021.115056.

[7] Bonnélye, V., Guey, L., Del Castillo, J., 2008. UF/MF as RO pre-treatment: the real benefit. Desalination 222, 59–65. https://doi.org/10.1016/j.desal.2007.01.129.

[8] Cui, X., Choo, K.-H., 2014. Natural organic matter removal and fouling control in low-pressure membrane filtration for water treatment. Environ Eng Res 19, 1–8. https://doi.org/10.4491/eer.2014.19.1.001.

[9] Li, L., Zhu, W., Zhang, P., Zhang, Z., Wu, H., Han, W., 2006. Comparison of AC/O3-BAC and O3-BAC processes for removing organic pollutants in secondary effluent. Chemosphere 62, 1514–1522. https://doi.org/10.1016/j.chemosphere.2005.06.043.

[10] Gnowe, W.D., Noubissié, E., Noumi, G.B., 2020. Influence of time and oxygenation on the degradation of organic matter, nitrogen and phosphates during the biological treatment of slaughterhouse effluent. Case Stud Chem Environ Eng 2, 100048. https://doi.org/10.1016/j.cscee.2020.100048.

[11] Zhang, H.-L., Jiang, W.-L., Liu, R., Zhou, Y., Zhang, Y., 2019. Organic degradation and extracellular products of pure oxygen aerated activated sludge under different F/M conditions. Bioresour Technol 279, 189–194. https://doi.org/10.1016/j.biortech.2019.01.130.

[12] P. van der Maas, E. Majoor, J.C. Schippers, Biofouling Control by Biological Activated Carbon Filtration: a Promising Method for WWTP Effluent Reuse, in: IWA Membrane Technology Conference, Beijiing, China, 2009.

[13] P. van der Maas, G. Veenendaal, J. Nonnekens, H. Brink, D. de Vogel, Biologische actiefkoolfiltratie met zuurstofdosering: veelbelovende techniek voor verwijdering geneesmiddelen?, H2O/Waternetwerk. (2020). ⟨https://www.h2owaternetwerk.nl/vakartikelen/biologische-actiefkoolfiltratie-met-zuurstofdosering-veelbelovende-techniek-voor-verwijdering-geneesmiddelen⟩.

[14] Rogowska, J., Cieszynska-Semenowicz, M., Ratajczyk, W., Wolska, L., 2020. Micropollutants in treated wastewater. Ambio 49, 487–503. https://doi.org/10.1007/s13280-019-01219-5.

[15] Verlicchi, P., Al Aukidy, M., Zambello, E., 2012. Occurrence of pharmaceutical compounds in urban wastewater: removal, mass load and environmental risk after a secondary treatment—a review. Sci Total Environ 429, 123–155. https://doi.org/10.1016/j.scitotenv.2012.04.028.

[16] Roccaro, P., 2018. Treatment processes for municipal wastewater reclamation: the challenges of emerging contaminants and direct potable reuse. Curr Opin Environ Sci Health 2, 46–54. https://doi.org/10.1016/j.coesh.2018.02.003.

[17] Simpson, D.R., 2008. Biofilm processes in biologically active carbon water purification. Water Res 42, 2839–2848. https://doi.org/10.1016/j.watres.2008.02.025.

[18] El Gamal, M., Mousa, H.A., El-Naas, M.H., Zacharia, R., Judd, S., 2018. Bio-regeneration of activated carbon: a comprehensive review. Gas Sep Purif 197, 345–359. https://doi.org/10.1016/j.seppur.2018.01.015.

[19] Aktaş, Ö., Çeçen, F., 2007. Bioregeneration of activated carbon: a review. Int Biodeterior Biodegrad 59, 257–272. https://doi.org/10.1016/j.ibiod.2007.01.003.

[20] Korotta-Gamage, S.M., Sathasivan, A., 2017. A review: potential and challenges of biologically activated carbon to remove natural organic matter in drinking water purification process. Chemosphere 167, 120–138. https://doi.org/10.1016/j.chemosphere.2016.09.097.

[21] Liu, C., Li, C., Shan, Y., Sun, Z., Chen, W., 2020. Comparison of two typical regeneration methods to the spent biological activated carbon in drinking water. Environ Sci Pollut Res 27, 16404–16414. https://doi.org/10.1007/s11356-019-07440-9.

[22] D. de Vogel, P. van der Maas, J. Kloosterman-Greftenhuis, S. Dost, Biologisch Actiefkoolfiltratie met Zuurstofdosering voor Verwijdering Miroverontreiningen uit RWZI-afvalwater, STOWA, 2020. https://www.stowa.nl/sites/default/files/assets/PUBLICATIES/Publicaties%202020/STOWA%2020200–46%20BODAC.pdf.

[23] Abromaitis, V., Racys, V., van der Marel, P., Meulepas, R.J.W., 2016. Biodegradation of persistent organics can overcome adsorption–desorption hysteresis in biological activated carbon systems. Chemosphere 149, 183–189. https://doi.org/10.1016/j.chemosphere.2016.01.085.

[24] Brunauer, S., Emmett, P.H., Teller, E., 1938. Adsorption of gases in multimolecular Layers. J Am Chem Soc 60, 309–319. https://doi.org/10.1021/ja01269a023.

[25] Seaton, N.A., Walton, J.P.R.B., quirke, N., 1989. A new analysis method for the determination of the pore size distribution of porous carbons from nitrogen adsorption measurements. Carbon 27, 853–861. https://doi.org/10.1016/0008-6223(89)90035-3.

[26] Borsje, C., Sleutels, T., Saakes, M., Buisman, C.J., Heijne, A., 2019. The granular capacitive moving bed reactor for the scale up of bioanodes. J Chem Technol Biotechnol 94, 2738–2748. https://doi.org/10.1002/jctb.6091.

[27] O'Toole, G.A., Pratt, L.A., Watnick, P.I., Newman, D.K., Weaver, V.B., Kolter, R., 1999. Genetic approaches to study of biofilms. Methods Enzym 310, 91–109. https://doi.org/10.1016/s0076-6879(99)10008-9.

[28] Christensen, G.D., Simpson, W.A., Younger, J.J., Baddour, L.M., Barrett, F.F., Melton, D.M., Beachey, E.H., 1985. Adherence of coagulase-negative staphylococci to plastic tissue culture plates: a quantitative model for the adherence of staphylococci to medical devices. J Clin Microbiol 22, 996–1006. https://doi.org/10.1128/jcm.22.6.996-1006.1985.

[29] Parada, A.E., Needham, D.M., Fuhrman, J.A., 2016. Every base matters: assessing small subunit rRNA primers for marine microbiomes with mock communities, time series and global field samples. Environ Microbiol 18, 1403–1414. https://doi.org/10.1111/1462-2920.13023.

[30] Quince, C., Lanzen, A., Davenport, R.J., Turnbaugh, P.J., 2011. Removing noise from pyrosequenced amplicons. BMC Bioinforma 12, 38. https://doi.org/10.1186/1471-2105-12-38.

[31] Bolyen, E., et al., 2019. Reproducible, interactive, scalable and extensible microbiome data science using QIIME 2. Nat Biotechnol 37, 852–857. https://doi.org/10.1038/s41587-019-0209-9.

[32] Callahan, B.J., McMurdie, P.J., Rosen, M.J., Han, A.W., Johnson, A.J.A., Holmes, S. P., 2016. DADA2: high-resolution sample inference from Illumina amplicon data. Nat Methods 13, 581–583. https://doi.org/10.1038/nmeth.3869.

[33] Quast, C., Pruesse, E., Yilmaz, P., Gerken, J., Schweer, T., Yarza, P., Peplies, J., Glöckner, F.O., 2013. The SILVA ribosomal RNA gene database project: improved data processing and web-based tools. Nucleic Acids Res 41, D590–D596. https://doi.org/10.1093/nar/gks1219.

[34] Bernstein, D.R., Glasgow, G.D.E., Lay, M.C., Manley-Harris, M., 2022. Accumulation of manganese oxides in biological activated carbon filters: implications for biodegradation studies. AWWA Water Sci 4, e1300. https://doi.org/10.1002/aws2.1300.

[35] Bruins, J.H., Petrusevski, B., Slokar, Y.M., Wübbels, G.H., Huysman, K., Wullings, B.A., Joris, K., Kruithof, J.C., Kennedy, M.D., 2017. Identification of the bacterial population in manganese removal filters. Water Supply 17, 842–850. https://doi.org/10.2166/ws.2016.184.

[36] Lee, S.-H., Nishijima, W., Lee, C.-H., Okada, M., 2003. Calcium accumulation on activated carbon deteriorates synthetic organic chemicals adsorption. Water Res 37, 4631–4636. https://doi.org/10.1016/S0043-1354(03)00425-1.

[37] Laurent, P., Kihn, A., Andersson, A., Servais, P., 2003. Impact of backwashing on nitrification in the biological activated carbon filters used in drinking water treatment. Environ Technol 24, 277–287. https://doi.org/10.1080/09593330309385560.

[38] Knappe, D.R.U., Snoeyink, V.L., Dagois, G., De Wolfe, J.R., 1992. Effect of calcium on thermal regeneration of GAC. J (Am Water Works Assoc) 84, 73–80.

[39] Wentzel, M.C., Mbewe, A., Ekama, G., 1995. Batch test for measurement of readily biodegradable COD and active organism concentrations in municipal waste waters. Water SA 21, 117–124.

[40] Benites-Zelaya, A.A., Soler-Cabezas, J.L., Ferrer-Polonio, E., Mendoza-Roca, J.A., Vincent-Vela, M.C., 2020. A step forward to the characterization of secondary effluents to predict membrane fouling in a subsequent ultrafiltration. Water 12, 1975. https://doi.org/10.3390/w12071975.

[41] Liu, C., Li, C., Shan, Y., Sun, Z., Chen, W., 2020. Comparison of two typical regeneration methods to the spent biological activated carbon in drinking water. Environ Sci Pollut Res 27, 16404–16414. https://doi.org/10.1007/s11356-019-07440-9.

[42] Li, X., Yuen, W., Morgenroth, E., Raskin, L., 2012. Backwash intensity and frequency impact the microbial community structure and function in a fixed-bed biofilm reactor. Appl Microbiol Biotechnol 96, 815–827. https://doi.org/10.1007/s00253-011-3838-6.

[43] How, S.W., Lim, S.Y., Lim, P.B., Aris, A.M., Ngoh, G.C., Curtis, T.P., Chua, A.S.M., 2018. Low-dissolved-oxygen nitrification in tropical sewage: an investigation on potential, performance and functional microbial community. Water Sci Technol 77, 2274–2283. https://doi.org/10.2166/wst.2018.143.

[44] Gerrity, D., Arnold, M., Dickenson, E., Moser, D., Sackett, J.D., Wert, E.C., 2018. Microbial community characterization of ozone-biofiltration systems in drinking water and potable reuse applications. Water Res 135, 207–219. https://doi.org/10.1016/j.watres.2018.02.023.

[45] LaPara, T.M., Hope Wilkinson, K., Strait, J.M., Hozalski, R.M., Sadowksy, M.J., Hamilton, M.J., 2015. The bacterial communities of full-scale biologically active, granular activated carbon filters are stable and diverse and potentially contain novel ammonia-oxidizing microorganisms. Appl Environ Microbiol 81, 6864–6872. https://doi.org/10.1128/AEM.01692-15.

[46] Palomo, A., Pedersen, A.G., Fowler, S.J., Dechesne, A., Sicheritz-Pontén, T., Smets, B.F., 2018. Comparative genomics sheds light on niche differentiation and the evolutionary history of comammox Nitrospira. ISME J 12, 1779–1793. https://doi.org/10.1038/s41396-018-0083-3.

[47] Ciancio Casalini, L., Piazza, A., Masotti, F., Garavaglia, B.S., Ottado, J., Gottig, N., 2022. Manganese oxidation counteracts the deleterious effect of low temperatures on biofilm formation in Pseudomonas sp. MOB-449. Front Mol Biosci 9, 1015582. https://doi.org/10.3389/fmolb.2022.1015582.

[48] Margot, J., Lochmatter, S., Barry, D.A., Holliger, C., 2016. Role of ammonia-oxidizing bacteria in micropollutant removal from wastewater with aerobic granular sludge. Water Sci Technol 73, 564–575. https://doi.org/10.2166/wst.2015.514.

[49] Rattier, M., Reungoat, J., Gernjak, W., Joss, A., Keller, J., 2012. Investigating the role of adsorption and biodegradation in the removal of organic micropollutants during biological activated carbon filtration of treated wastewater. J Water Reuse Desalin 2, 127–139. https://doi.org/10.2166/wrd.2012.012.

[50] Rattier, M., Reungoat, J., Keller, J., Gernjak, W., 2014. Removal of micropollutants during tertiary wastewater treatment by biofiltration: role of nitrifiers and removal mechanisms. Water Res 54, 89–99. https://doi.org/10.1016/j.watres.2014.01.030.

[51] Krishnan, R.Y., Manikandan, S., Subbaiya, R., Biruntha, M., Govarthanan, M., Karmegam, N., 2021. Removal of emerging micropollutants originating from pharmaceuticals and personal care products (PPCPs) in water and wastewater by advanced oxidation processes: a review. Environ Technol Innov 23, 101757. https://doi.org/10.1016/j.eti.2021.101757.

[52] Men, Y., Achermann, S., Helbling, D.E., Johnson, D.R., Fenner, K., 2017. Relative contribution of ammonia oxidizing bacteria and other members of nitrifying activated sludge communities to micropollutant biotransformation. Water Res 109, 217–226. https://doi.org/10.1016/j.watres.2016.11.048.

[53] Tran, T.N., Kim, D.-G., Ko, S.-O., 2018. Synergistic effects of biogenic manganese oxide and Mn(II)-oxidizing bacterium Pseudomonas putida strain MnB1 on the degradation of 17 α-ethinylestradiol. J Hazard Mater 344, 350–359. https://doi.org/10.1016/j.jhazmat.2017.10.045.

[54] Wang, G., Hambly, A.C., Dou, Y., Wang, G., Tang, K., Andersen, H.R., 2022. Polishing micropollutants in municipal wastewater, using biogenic manganese

oxides in a moving bed biofilm reactor (BioMn-MBBR. J Hazard Mater 427, 127889. https://doi.org/10.1016/j.jhazmat.2021.127889.
[55] Daims, H., Nielsen, J.L., Nielsen, P.H., Schleifer, K.-H., Wagner, M., 2001. In situ characterization of *Nitrospira* -like nitrite-oxidizing bacteria active in wastewater treatment plants. Appl Environ Microbiol 67, 5273–5284. https://doi.org/10.1128/AEM.67.11.5273-5284.2001.
[56] Bock, E., Wagner, M., 2006. Oxidation of inorganic nitrogen compounds as an energy source. In: Dworkin, M., Falkow, S., Rosenberg, E., Schleifer, K.-H., Stackebrandt, E. (Eds.), The Prokaryotes. Springer, New York, New York, NY, pp. 457–495. https://doi.org/10.1007/0-387-30742-7_16.
[57] Law, Y., Matysik, A., Chen, X., Swa Thi, S., Ngoc Nguyen, T.Q., Qiu, G., Natarajan, G., Williams, R.B.H., Ni, B.-J., Seviour, T.W., Wuertz, S., 2019. High dissolved oxygen selection against *Nitrospira* sublineage I in full-scale activated sludge. Environ Sci Technol 53, 8157–8166. https://doi.org/10.1021/acs.est.9b00955.
[58] Prosser, J.I., Head, I.M., Stein, L.Y., 2014. The family nitrosomonadaceae. In: Rosenberg, E., DeLong, E.F., Lory, S., Stackebrandt, E., Thompson, F. (Eds.), The Prokaryotes. Springer Berlin Heidelberg, Berlin, Heidelberg, pp. 901–918. https://doi.org/10.1007/978-3-642-30197-1_372.
[59] Gebers, R., 1981. Enrichment, isolation, and emended description of pedomicrobium ferrugineum aristovskaya and pedomicrobium manganicum aristovskaya. Int J Syst Bacteriol 31, 302–316. https://doi.org/10.1099/00207713-31-3-302.
[60] Tyler, P.A., 1970. Hyphomicrobia and the oxidation of manganesse in aquatic ecosystems. Antonie Van Leeuwenhoek 36, 567–578. https://doi.org/10.1007/BF02069059.
[61] Molari, M., Janssen, F., Vonnahme, T.R., Wenzhöfer, F., Boetius, A., 2020. The contribution of microbial communities in polymetallic nodules to the diversity of the deep-sea microbiome of the Peru Basin (4130–4198\,m depth). Biogeosciences 17, 3203–3222. https://doi.org/10.5194/bg-17-3203-2020.
[62] Nealson, K.H., Tebo, B.M., Rosson, R.A., 1988. Occurrence and mechanisms of microbial oxidation of manganese. In: Advances in Applied Microbiology. Elsevier, pp. 279–318. https://doi.org/10.1016/S0065-2164(08)70209-0.
[63] Sjöberg, S., Stairs, C.W., Allard, B., Homa, F., Martin, T., Sjöberg, V., Ettema, T.J. G., Dupraz, C., 2020. Microbiomes in a manganese oxide producing ecosystem in the Ytterby mine, Sweden: impact on metal mobility. FEMS Microbiol Ecol 96, fiaa169. https://doi.org/10.1093/femsec/fiaa169.
[64] Carmichael, S.K., Bräuer, S.L., 2015. 7. Microbial diversity and manganese cycling: a review of manganese-oxidizing microbial cave communities. In: Summers Engel, A. (Ed.), Microbial Life of Cave Systems. DE GRUYTER, pp. 137–160. https://doi.org/10.1515/9783110339888-009.
[65] Hohle, T.H., O'Brian, M.R., 2012. Manganese is required for oxidative metabolism in unstressed Bradyrhizobium japonicum cells: manganese-dependent metabolism in B. japonicum. Mol Microbiol 84, 766–777. https://doi.org/10.1111/j.1365-2958.2012.08057.x.
[66] Yu, H., Leadbetter, J.R., 2020. Bacterial chemolithoautotrophy via manganese oxidation. Nature 583, 453–458. https://doi.org/10.1038/s41586-020-2468-5.
[67] Jones, D., Lyon, E., Macalady, J., 2008. Geomicrobiology of biovermiculations from the Frasassi Cave System, Italy. J Cave Karst 70.
[68] Cao, L.T.T., Kodera, H., Abe, K., Imachi, H., Aoi, Y., Kindaichi, T., Ozaki, N., Ohashi, A., 2015. Biological oxidation of Mn(II) coupled with nitrification for removal and recovery of minor metals by downflow hanging sponge reactor. Water Res 68, 545–553. https://doi.org/10.1016/j.watres.2014.10.002.
[69] Vandenabeele, J., Vande Woestyne, M., Houwen, F., Germonpré, R., Vandesande, D., Verstraete, W., 1995. Role of autotrophic nitrifiers in biological manganese removal from groundwater containing manganese and ammonium. Micro Ecol 29. https://doi.org/10.1007/BF00217425.
[70] Du, X., Liu, G., Qu, F., Li, K., Shao, S., Li, G., Liang, H., 2017. Removal of iron, manganese and ammonia from groundwater using a PAC-MBR system: the anti-pollution ability, microbial population and membrane fouling. Desalination 403, 97–106. https://doi.org/10.1016/j.desal.2016.03.002.
[71] McCormick, N.E., Earle, M., Ha, C., Hakes, L., Evans, A., Anderson, L., Stoddart, A. K., Langille, M.G.I., Gagnon, G.A., 2021. Biological and physico-chemical mechanisms accelerating the acclimation of Mn-removing biofilters. Water Res 207, 117793. https://doi.org/10.1016/j.watres.2021.117793.
[72] Teng, Y., Wang, X., Li, L., Li, Z., Luo, Y., 2015. Rhizobia and their bio-partners as novel drivers for functional remediation in contaminated soils. Front Plant Sci 6. https://doi.org/10.3389/fpls.2015.00032.
[73] Huang, X., Geng, M., Wang, K., He, Y., Li, G., Feng, C., Shi, B., 2023. Suppression of performance of activated carbon filter due to residual aluminum accumulation. J Hazard Mater 445, 130637. https://doi.org/10.1016/j.jhazmat.2022.130637.
[74] Li, H., Fu, B., Huang, H., Wu, S., Ge, J., Zhang, J., Li, F., Qu, P., 2022. Catalytic degradation of organic pollutants by manganese oxides: a comprehensive review. Environ Pollut Bioavailab 34, 395–406. https://doi.org/10.1080/26395940.2022.2123047.
[75] Ning, R., 2009. Colloidal iron and manganese in water affecting RO operation. Desalin Water Treat - Desalin Water Treat 12, 162–168. https://doi.org/10.5004/dwt.2009.918.
[76] Castaño Osorio, S., Biesheuvel, P.M., Spruijt, E., Dykstra, J.E., van der Wal, A., 2022. Modeling micropollutant removal by nanofiltration and reverse osmosis membranes: considerations and challenges. Water Res 225, 119130. https://doi.org/10.1016/j.watres.2022.119130.